JACS
JOURNAL OF THE AMERICAN CHEMICAL SOCIETY

ARTICLE

pubs.acs.org/JACS

# Reaction Dynamics of a Molecular Switch Unveiled by Coherent Two-Dimensional Electronic Spectroscopy

Martin Kullmann, Stefan Ruetzel, Johannes Buback, Patrick Nuernberger, and Tobias Brixner*

Institut für Physikalische und Theoretische Chemie, Universität Würzburg, Am Hubland, 97074 Würzburg, Germany

**ABSTRACT:** Coherent two-dimensional electronic spectroscopy is usually employed on molecular species with fixed geometric configuration. Here we present two-dimensional Fourier-transform electronic spectra of dissolved 6,8-dinitro-1′,3′,3′-trimethylspiro[2*H*-1-benzopyran-2,2′-indoline] (6,8-dinitro-BIPS), a photochromic system present in two ring-open forms differing in the cis/trans configuration of a double bond, which both undergo a photoinduced ring closure. The two-dimensional spectra, recorded with 20 fs pump pulses centered at 605 nm and a supercontinuum probe covering the complete visible spectral range, allow for a detailed analysis of the photophysics and photochemistry of the two isomers and directly reveal that cis/trans isomerization among them does not play a major role. This experiment demonstrates the potential of two-dimensional electronic spectroscopy for reactive processes.

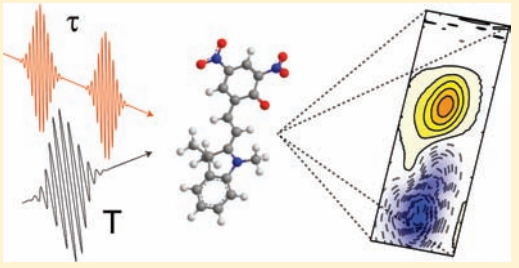


## INTRODUCTION

Photochromic compounds are promising molecular systems for organic electronic devices such as ultrafast transistors because of their unique ability to be switchable between two stable states with light.[1] 6,8-dinitro-BIPS[2,3] is a merocyanine-spiropyran system based on a 6$\pi$-electrocyclic reaction which can be switched in both directions with good yield and high speed.[4,5] The ring-closed spiropyran comprises two orthogonal chromophores (pyran and indole moieties) which do not absorb in the visible spectral range, whereas the ring-open merocyanine consists of one large planar $\pi$ system strongly absorbing in the visible spectral range. There are two stable ring-open merocyanine isomers with differing cis/trans configurations present at room temperature, which also exhibit different photochemical dynamics, but in contrast to other systems based on a 6$\pi$-electrocyclic reaction the photochemical ring closure is accessible by both isomers. In an efficient switching device, however, interconversion of the ring-open isomers as a competitive reaction path to ring closure is disadvantageous.

In a series of transient-absorption experiments, we could infer, after analyzing many overlapping signals and applying various reaction models, that the photoisomerization yield is below 2%.[5] Two-dimensional (2D) spectroscopy[6−10] can provide a more versatile and illustrative approach, as it directly relates the excitation dependence and the spectral response of a system within a single measurement. This allows for resolving the spectral behavior and the interconnection of participating states. Coherent 2D spectroscopy has been implemented in different wavelength regimes. The infrared variant (2DIR) enables analysis of the electronic ground-state behavior and the couplings between different vibrational states.[11,12] For electronic correlations 2D spectroscopy was realized in the visible[13−16] and the ultraviolet (UV)[17,18] spectral range.

Apart from the application to purely photophysical processes 2D experiments on chemical nonequilibrium systems have also been realized. In transient 2DIR spectroscopy, a preceding (visible or UV) pump pulse triggers a chemical process, e.g. the switching process in peptides,[19,20] unfolding dynamics in proteins,[21] metal-to-ligand charge transfer,[22] or bond cleavage in metal carbonyls.[23] In 2DIR triggered-exchange spectroscopy, this additional pump pulse starts the reaction after the IR excitation, linking vibrations in the reactant to those in the product.[22,23] The molecules can also undergo a structural change between the excitation and detection steps without a further triggering pulse (2DIR exchange spectroscopy).[24−28] In this publication, we transfer this concept from vibrational to electronic 2D spectroscopy. This allows us to follow the chemical reaction dynamics of two possibly interconverting molecular species in electronically excited states.

We employ 2D electronic spectroscopy in pump−probe geometry[29] with inherently phase-stable pump-pulse pairs, generated and delayed with a femtosecond pulse shaper,[10,30−33] and a supercontinuum probe.[34] The first pump pulse interacts with the sample in the electronic ground state, followed by a second pump pulse, phase stabilized relative to the first one, after the coherence time $\tau$. After a waiting time $T$ the probe pulse brings the system into a coherent superposition of states. The emitted response is heterodyned by the probe and measured in a spectrally resolved manner. Fourier transformation along $\tau$ yields the electronic 2D spectrum.

Figure 1a illustrates the absorption spectrum of the open form of 6,8-dinitro-BIPS (black/gray) which comprises a broad absorption band in the visible spectral range ($\nu_{max}$ = 540 THz, $\lambda_{max}$ = 560 nm). Two isomers (Figure 1a, right) exist, predominantly the TTC configuration (red) and (about 1 order of magnitude less) the TTT configuration (blue), absorbing at 540 THz (560 nm) and 490 THz (600 nm), respectively.[4,5] The labels T and C refer

**Received:** April 7, 2011
**Published:** August 02, 2011

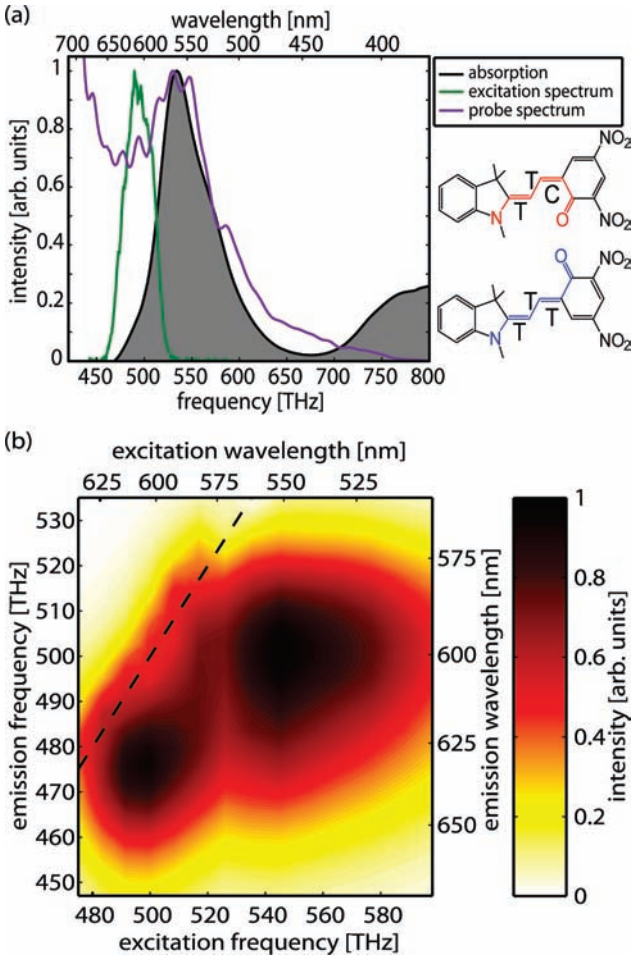


**Figure 1.** (a) Normalized absorption spectrum of 6,8-dinitro-BIPS dissolved in chloroform (black/gray) and experimental spectra of pump (green) and probe (purple) pulses. The two ring-open isomers TTC (red) and TTT (blue) are shown on the right-hand side. (b) Excitation-dependent fluorescence spectrum substantiating the existence of two different isomers. The black dashed line represents the diagonal.

to the trans or cis configuration of the bonds in the methine bridge, as shown at the right of Figure 1a. We adjusted the center wavelength of the laser to 605 nm (green) to excite roughly the same amount of both isomers. The probe continuum (purple) covers the complete visible spectral range. Both isomers undergo a ring-closure reaction after excitation, with quantum efficiencies of 40% (TTC) and 35% (TTT).[4,5] The excitation-frequency-dependent fluorescence clearly shifts from around 475 THz to 500 THz with increasing excitation frequency, as shown in Figure 1b. Thus, each isomer can (for example) be identified by the corresponding stimulated-emission signal in our experiments.

Possible reaction schemes and corresponding schematic 2D spectra are depicted in Figure 2. Expected signals are numbered 1−7, as indicated in the 2D spectrum in the upper left. After excitation to the $S_1$ state both isomers (TTC and TTT) undergo a ring-closure reaction to spiropyran (SP). The diagonal signals are due to ground-state absorption (GSA). According to Figure 1, the GSA of TTT (signal 5) is slightly red-shifted compared to that of TTC (signal 4). The same is the case for the off-diagonal contributions arising from stimulated emission (SE) out of each individual isomer (signal 6 for TTC, signal 7 for TTT). Each SE signal has to appear vertically displaced from the respective GSA signal, and the spectral difference along the probe frequency is a consequence of Figure 1b. Excited-state absorption (ESA) appears for both isomers and has to be shifted vertically upward with respect to GSA because the ESA is blue-shifted relative to the GSA. TTT exhibits two transitions instead of one for TTC to higher-lying states, and the TTT signals are again red-shifted with respect to TTC (signal 1 for TTC, signals 2 and 3 for TTT).[4,5]

We now discuss three scenarios of possible chemical reaction pathways: no isomerization between TTC and TTT (Figure 2a), isomerization during relaxation to the ground state via a conical intersection connecting $S_1$ and $S_0$ merocyanine potential energy surfaces (Figure 2b), and isomerization in the excited state passing an isomerization barrier in $S_1$ connecting parts of the potential energy surfaces belonging to TTT and TTC (Figure 2c). Schematics of the 2D absorptive spectra are shown in the right column of Figure 2 for early ($T > 0$) and longer waiting times ($T \gg 0$). If no isomerization occurs, the two chemical systems TTC and TTT are separated and thus any 2D peak can only arise at the crossing between lines of the same color in Figure 2 (either red/red or blue/blue). If, on the other hand, the two species interconvert, 2D peaks may also arise at red/blue crossings, since they originate from one isomer and end up in the other isomer.

More specifically, if no isomerization occurs, only the cross peaks belonging to ESA and SE will show up, and for $T \gg 0$, only the photobleach (indicating SP product formation) at the GSA frequencies will remain (Figure 2a). If ultrafast isomerization directly to the ground state takes place, additional positive cross peaks (indicated by filled circles) will appear in the GSA region of both isomers shortly after excitation and will remain for $T \gg 0$ (Figure 2b) because the amount of TTC and TTT after excitation of the other isomer would be higher, resulting in increased off-diagonal absorption. In the case of isomerization in the excited state, new cross peaks in the SE region (negative) and in the ESA region (positive) of the other respective isomer will emerge for $T > 0$ (Figure 2c) because after the initial excitation of TTT (vertical blue line) the relaxation would happen alongside the photochemical channels of TTC (horizontal red lines) and vice versa. After relaxation, these give rise to positive cross peaks in the GSA region for $T \gg 0$. The idea is now to find out which of the three scenarios is correct by comparing measured 2D spectra with the schematic illustrations in Figure 2. In this comparison, one has to keep in mind that experimental 2D spectra may exhibit broad and overlapping contributions, complicating the identification of isomerization peaks. The measured 2D spectra also reflect the shape of the excitation and probe laser spectra (Figure 1), which can lead to an apparent shift in peak positions.

## EXPERIMENTAL SECTION

6,8-dinitro-BIPS was synthesized according to the literature[35] via the Knoevenagel condensation reaction of commercially available 1,2,3,3-tetramethyl-3*H*-indolium and 3,5-dinitrosalicylaldehyde, resulting in the merocyanine form of 6,8-dinitro-BIPS in 79% yield, and characterized by HPLC and 400 MHz NMR spectroscopy.[4]

Steady-state absorption spectra in the visible spectral range were measured in a 2 mm suprasil cuvette with a Hitachi U-2000 spectrophotometer. Fluorescence spectra were recorded with a Jasco FP-6300 fluorescence spectrometer in a 1 cm flow cell. The depicted spectrum consists of the fluorescence of merocyanine minus a pure solvent measurement in order to reduce stray light alongside the diagonal. All spectra were recorded directly after solving the crystals in chloroform.

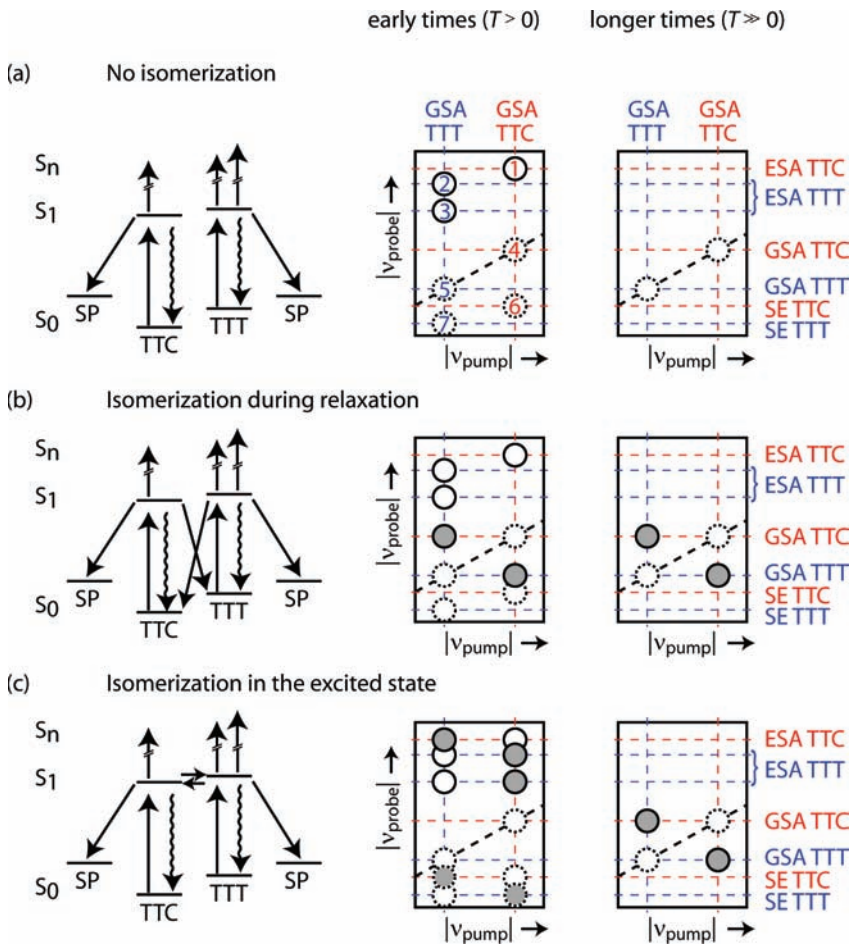


**Figure 2.** Possible reaction and isomerization schemes of 6,8-dinitro-BIPS isomers TTC and TTT from the ring-open form to the closed spiropyran (SP) and schematics of the corresponding 2D spectra (TTC, red dashed lines; TTT, blue dashed lines). Solid circles illustrate positive values corresponding to increased absorption and dashed circles negative contributions resulting from decreased transient absorption. Additional isomerization cross peaks are indicated by gray filled circles located at an intersection of a blue and a red line. (a) If no isomerization occurs, no isomerization cross peaks emerge in the corresponding 2D spectrum, neither at early ($T > 0$, left) nor at longer waiting times ($T \gg 0$, right). The spectrum for early times depicts the numbering of the expected signals for further discussions. (b) If isomerization occurs during relaxation to the ground state, isomerization peaks will appear in the region of the GSA for $T > 0$ and will remain for $T \gg 0$. (c) In the case of isomerization in the excited state, there will be isomerization peaks in the region of the ESA and SE for $T > 0$ that will appear in the region of the GSA for $T \gg 0$.

For the 2D measurements a partially collinear, pulse-shaper-assisted approach in pump−probe geometry was used.[30−33,36] A Ti:sapphire oscillator and regenerative amplifier (Solstice, Spectra Physics) with output pulses centered at 800 nm with 100 fs duration and 1 kHz repetition rate seeds the generation of the visible pump and probe pulses. The visible pump pulses centered at 500 THz (605 nm) with 20 fs duration were generated in a noncollinear optical parametric amplifier (TOPAS White, Light Conversion). These pulses were compressed and split into phase-stable double pulses with adjustable time delay $\tau$ by a LCD-based femtosecond pulse shaper and characterized via pulse-shaper-assisted collinear frequency-resolved optical gating (cFROG).[37,38] The two-layer, 640-pixel mask (SLM-640, CRI) of the broad-band shaper allows for independent amplitude and phase shaping, resulting in pulses with about 200 nJ of energy. The additional adjustable delay $T$ between the second pulse and the probe pulse was introduced by a mechanical stage with a length of 600 mm. The supercontinuum probe pulses ranging from 420 THz to 820 THz (corresponding to 370−710 nm) were generated by focusing a small portion of the 800 nm pulses into a linearly moving $CaF_2$ plate. The pump and probe pulses had parallel polarization and were spatially overlapped in a 200 $\mu$m flow cell containing a 0.5 mM solution of 6,8-dinitro-BIPS in chloroform.

The measurement of changes in the optical density of the sample introduced by the pump pulses was carried out with 1 kHz acquisition rate by blocking every second pair of pulse-shaper-generated double pulses. In this way all spectra are spectrally normalized to the white-light spectrum of the probe pulse as in conventional transient-absorption experiments. The two-dimensional data recording was done with a four-step phase-cycling technique which effectively eliminates the pump−probe contribution in the signal and reduces pump-induced scatter.[17,31,32,36] Combining these four data sets, as described in the literature,[36] before Fourier transformation along $\tau$ and taking the real part of the data give us the automatically phased 2D absorptive spectra.

## RESULTS

The real parts of the experimental electronic 2D spectra of 6,8-dinitro-BIPS dissolved in chloroform are shown in parts a−f of Figure 3 for waiting times of $T$ = 3, 30, 100, 300, 1000, and 3000 ps, respectively. The diagonal is indicated by the black dashed line. Positive values (reddish colors) describe increased absorption, and negative values (bluish colors) correspond to a decreased absorption change of the probe pulse. Vertical grid

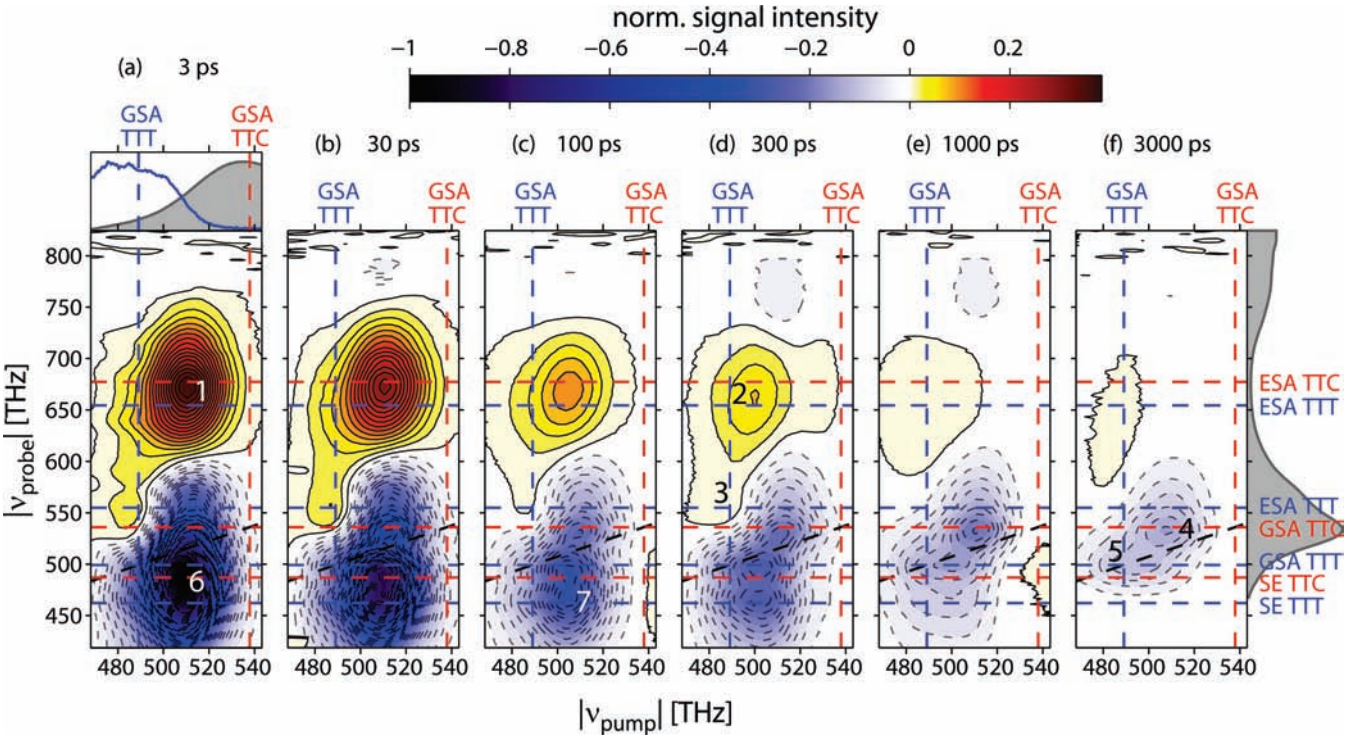


**Figure 3.** Absorptive 2D electronic spectra of 6,8-dinitro BIPS dissolved in chloroform for waiting times of (a) 3, (b) 30, (c) 100, (d) 300, (e) 1000, and (f) 3000 ps. The frequencies of GSA, SE, and ESA are indicated by red dashed lines for TTC and by blue dashed lines for TTT. Positive values (yellow, red) describe increased values of absorption, and negative values (blue, black) correspond to decreased transient absorption. Contour lines are drawn in equally spaced intervals with 60 levels, where solid (dashed) lines indicate positive (negative) values. All spectra were normalized relative to the minimum of the 3 ps spectrum, corresponding to an absorption change of −1. The contributions are numbered where they are unambiguously identified. The spectrum of the pump pulses (blue) is shown on top of spectrum (a) for further clarification in addition to the merocyanine absorption spectrum (black/gray), which is also shown on the right side of spectrum (f).

lines indicate GSA frequencies of TTC (red) and TTT (blue) and horizontal grid lines frequencies of GSA, ESA, and SE of both isomers, as labeled. The corresponding expected frequencies have been assigned by global fitting routines of transient-absorption data.[5] As can be seen in Figure 1 and the upper part of Figure 3a, the pump−pulse spectrum only partially overlaps with the absorption spectrum. Note that this shifting toward red frequencies was done in order to excite both isomers substantially, despite their different concentrations in thermodynamic equilibrium. As a consequence, the major contributions of the TTC isomer are not observed on the vertical red line indicating the maximum of the GSA of TTC but are shifted to lower pump frequencies of about 515 THz. Nevertheless, this contribution is clearly identified via the horizontal red line indicating TTC GSA at 540 THz (see position of signal 4 in Figure 3f).

After 3 ps the 2D spectrum at lower probe frequencies is dominated by the SE of TTC (signal 6). At higher probe frequencies, one observes ESA located at the frequency corresponding to TTC (signal 1). ESA is also observed for probe frequencies down to about 525 THz, but only at low pump frequencies (near the GSA of TTT), as expected due to the existence of the two ESA signals of TTT (signals 2 and 3). The low-energy ESA band (signal 3) becomes evident in particular for $T$ = 30 and 300 ps due to the curvature of the contour lines, indicating two different but overlapping bands, not a single broad contribution. In the 2D spectrum for $T$ = 3 ps, oscillations along the probe axis are visible in the ESA (at lower pump frequencies) that are related to Raman-active modes of the solvent and the chirp of the supercontinuum probe,[39−41] since $T$ slightly varies for different values of $\nu_{probe}$ by virtue of this chirp. However, signals due to Raman modes are no longer observed after a few picoseconds, which is significantly shorter than the relaxation times of excited 6,8-dinitro-BIPS back to the ground state. Second-order and third-order dispersion of the probe continuum were determined as 300 fs$^2$ and 130 fs$^3$, respectively, and do not play a major role for long waiting times due to the relatively large time constants of the investigated system.[42]

## ■ DISCUSSION

One approach to investigate the role of the isomers and their photoinduced behavior with 2D spectroscopy could be to decompose the data into decay-associated 2D spectra.[33] Here, we combine a series of 2D electronic spectra with the information on the photodynamics obtained in transient absorption studies, where we determined strongly differing excited-state lifetimes of 95 ps for TTC and 900 ps for TTT.[4,5] Hence, the ESA shifts to lower pump frequencies during the first 300 ps (Figure 3a−d) and a weak ESA contribution of TTT is remaining after 3000 ps (f). For $T$ = 3000 ps, signals 4 and 5 originating from GSA of TTC and TTT, respectively, are observed, which persist due to the absence of merocyanine and the formation of ring-closed SP. SE for TTC (signal 6) initially disappears, leading to the dominant contribution of TTT in the region of SE after 300 ps (signal 7). A separation of TTT GSA (signal 5) and TTC SE (signal 6), both peaking around 500 THz (600 nm) (compare

the linear absorption and fluorescence spectra in Figure 1), is possible when we take the temporal behavior into account. Up to $T$ = 100 ps, TTC behavior dominates while TTT contributions remain nearly unchanged with a decay of only 10%. This allows for the assignment of the intense negative features at 500 THz to $S_1$ emission of TTC in Figure 3a,b. For larger $T$ the behavior of the TTT GSA is visible. This distinction is also possible considering the TTC ground-state bleach (signal 4) which remains nearly unchanged in Figure 3c−f, thus proving that the photochemical reaction of TTC is over. Another evidence for the different dynamics of both isomers is the slight shift of the strong negative feature consisting of TTC SE, TTT GSA, and TTT SE: for small values of $T$, it is mainly due to TTC SE (signal 6), whereas for large $T$, it is due to the bleach of TTT (signal 5). This is directly evidenced by a shift on the pump axis from 515 THz as center frequency to 500 THz: i.e., from the energetically higher TTC transition to the slightly energetically lower TTT transition. In the 2D spectrum for $T$ = 300 ps, one can even clearly separate these three negative, partially overlapping features 4, 5, and 7, which belong to the bleach of TTC and TTT and the SE of TTT, respectively. A negative contribution for probe frequencies above 720 THz, best seen for $T$ = 300 and 1000 ps, can be assigned to the bleach of the second merocyanine absorption band extending from 670 THz (450 nm) into the UV (as visible in Figure 1 and to the right of Figure 3f).

After having discussed all features of the 2D spectra, we now take into account the isomerization schemes of Figure 2 for interpretation. Basically, all schemes comprise a set of seven peaks, corresponding to ESA, GSA, and SE unique for each isomer and a set of off-diagonal peaks centered at crossings of TTC and TTT frequencies. If the isomerization between both isomers happens in the excited state (Figure 2c), five additional isomerization peaks for $T \leq$ 100 ps are expected in the corresponding 2D spectra of Figure 3. The negative contributions in the expected 2D spectra for $T$ = 3 and 30 ps are dominated by the strong SE of TTC, but for $T$ = 100 ps three contributions belonging to SE (signal 7) and GSA (signal 5) of TTT and GSA of TTC (signal 4) are identified. These signals also dominate the $T$ = 300 ps spectrum; no additional features emerge. Further information is provided by the positive ESA: the only detectable features are the expected frequency shift with increasing $T$ (since TTC decays faster than TTT) and the overall decay due to relaxation to the ground state. The absence in the experimental spectra of clear isomerization peaks or strong disturbances as marked in Figure 2c by the filled gray circles rules out a reaction pathway with high quantum yield between the isomers in the excited state.

The very small yield or the nonexistence of isomerization can be explained by the existence of a barrier between TTT and TTC excited-state potential minima. Barriers in the excited state are well-known for merocyanines, as shown via theoretical calculations for merocyanines without ring-closure capability.[43] Additionally, a merocyanine-spiropyran model neglecting the indole and any substituents was used in order to explore theoretically the ring closure via conical intersections. Barriers, connecting different isomers, and a fast pathway to a ring-closed form were found.[44] The barrier heights were estimated to be around 0.5 eV. While this study assumed $S_2$ excitation which would enable the passing of the barrier with the help of excess energy, direct excitation into $S_1$ basically reduces the available energy, possibly hindering the isomerization. We can transfer these findings to the related but not identical 6,8-dinitro-BIPS. This could explain the negligible TTC/TTT isomerization in the excited state, because the pump pulses centered at 500 THz possess only an energetic window of 2.05 ± 0.15 eV and are not sufficient to make the crossing of such a high barrier likely. Another indication for why isomerization is absent is gained by comparing the transient-absorption studies for 6-nitro-BIPS[45] and our previous results on 6,8-dinitro-BIPS.[5] For 6-nitro-BIPS wavelength-selective excitation yields differing outcomes regarding isomerization, dependent on the pump wavelength. One of the two merocyanine isomers, present after continuous UV excitation of the thermally stable spiropyran, changes only the first stereoconfiguration in the methine bridge from trans to cis after excitation in the visible. The second isomer is additionally capable of isomerization to the other present isomer, if enough excess energy is available by exciting it on the blue edge of its absorption band. However, no ring closure is detectable for this system. For 6,8-dinitro-BIPS the second nitro group affects the potential energy surfaces in such a way that merocyanine isomers are thermally more stable than spiropyran and photochemical ring closure becomes accessible, which is very rare for merocyanines. Variation of the excitation wavelength changes only the relative amount of excitation of the two isomers, but no impact of the excess energy on photoisomerization capabilities is visible. It is plausible to ascribe the negligible isomerization to the existence of energetically preferred ring-closure pathways and higher barriers between the isomers, since the photochemistry changes quite radically due to the substituents.

After having discussed and excluded isomerization through the excited state, we now consider isomerization during relaxation to the merocyanine ground state via conical intersections connecting TTC and TTT in $S_1$ and $S_0$ (see Figure 2b). This would result in positive contributions to the 2D spectra in off-diagonal areas where GSA lines of both isomers intersect. Straightforward insight is gained for the waiting time $T$ = 3000 ps: no isomerization peaks (located at the gray filled circles in Figure 2b) or strong positive disturbances in the contour lines are visible in the vicinity of the experimental GSA of both molecules (signals 4 and 5), and hence isomerization between TTC and TTT during relaxation can also be ruled out as an important reaction pathway. This is again in accordance with ref 43, which compares the excited states of merocyanines, cyanines, and polyenes. While polyenes possess a biradicaloid structure, an even number of $\pi$ orbitals in the excited state, and conical intersections between $S_1$ and $S_0$, the excited states of cyanines have charge-transfer character and an odd number of $\pi$ orbitals. Merocyanine shares the latter properties, and the calculations for the merocyanine structure in ref 43 show a very high barrier hindering photoisomerization via crossing of a conical intersection, if such a conical intersection exists at all. Thus, the minor contribution or nonexistence of isomerization to the photoreaction pathways for 6,8-dinitro-BIPS by passing a conical intersection in $S_1$ seems plausible.

Hence, the 2D spectroscopy data are in accordance with the simplest model (Figure 2a), which does not involve any photoisomerization between the two merocyanine isomers. For $T > 0$ three positive (signals 1−3) and four negative peaks (signals 4−7) are expected, which are all evident in our data as discussed above. For $T \gg 0$, when the ground-state relaxation is over, only the permanent bleach should remain in our data. Since this is the case (with some TTT still in the excited state in the $T$ = 3000 ps spectrum), the reaction scheme in Figure 2a is the most probable one. No isomerization cross peaks or even distinct deformations are observed, substantiating that indeed isomerization does not play a major role in the photochemistry of 6,8-dinitro-BIPS.

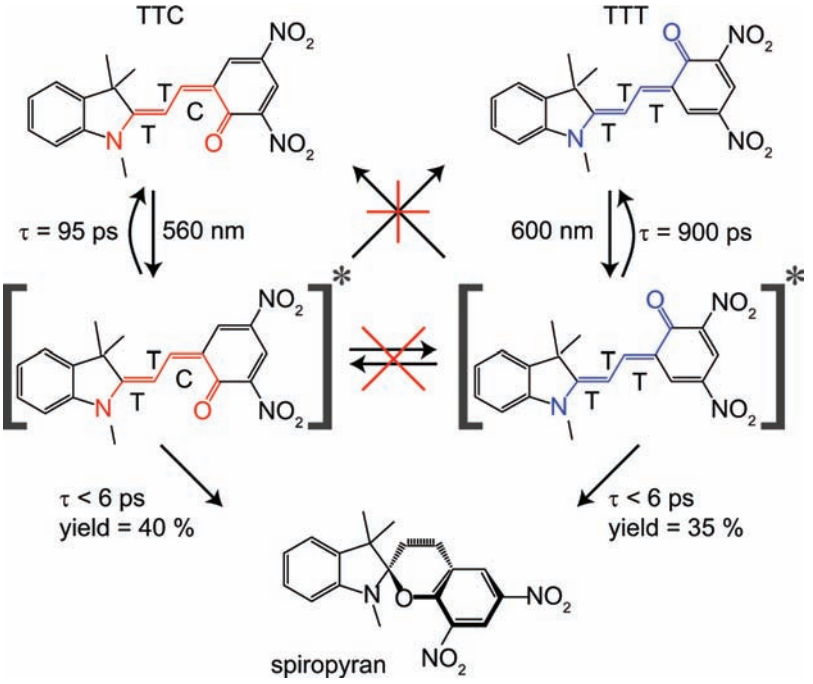


**Figure 4.** Photochemical reaction scheme of 6,8-dinitro-BIPS consisting of two merocyanine isomers (TTC and TTT) in the ground state (top row), their excited states (middle row), and the spiropyran product (bottom). As evidenced in this publication, isomerization pathways can be excluded as major channels (red crosses). The remaining reactions (black arrows) are reactions back to the corresponding ground state via stimulated emission or fluorescence with 95 ps/900 ps (TTC/TTT) and ring closure to spiropyran on a picosecond time scale.

Isomerization with very low quantum yields (compare the upper boundary of 2% determined indirectly in ref 5), however, would cause a very slight contour-line deformation, which cannot be ruled out with absolute certainty.

We now summarize the results of the present study within the reaction scheme of 6,8-dinitro-BIPS in Figure 4. We can exclude pronounced cis/trans isomerization (red crosses); as a result, only the reaction pathways shown take place. Thus, after photoexcitation both isomers partially undergo a ring closure to the identical spiropyran form with yields of 35−40%, possibly through a conical intersection, while the remaining part of the excited molecules return to their corresponding ground state via fluorescence. As a result, the photochemical fate of the excited merocyanine is determined in the first few picoseconds, with the alternatives of either ring closure or fluorescence back to the corresponding ground state.

## SUMMARY

We have used 2D electronic spectroscopy to examine the photochemical behavior of the molecular switch 6,8-dinitro-BIPS. Two merocyanine isomers were present in solution, featuring differing relaxation characteristics, which is directly evident in the 2D spectra. The probe pulse covering the complete visible spectral range allowed us to simultaneously monitor temporal changes over a broad spectral region. A considerable frequency shift in the ESA could be identified, due to the differing time constants of the two isomers. Whereas the linear spectra corresponding to the GSA and SE of both isomers strongly overlap, the corresponding peaks in the 2D spectra could be clearly distinguished. The absence of cross peaks connecting TTC and TTT in the spectra corroborates that cis/trans photoisomerization between the two isomers is a negligible reaction channel. Hence, by means of broad-band coherent two-dimensional electronic spectroscopy we could directly visualize the excited-state and relaxation dynamics of a complex photoreactive molecular system.

Conventional pump−probe spectroscopy on multichannel reactive systems[4,5] may require tedious and elaborate data analysis of many different data sets and combination of those results to retrieve information about the relevant pathways in an indirect procedure. If spectroscopic signatures from the involved species overlap significantly in the transient spectra, it may even not be possible at all to disentangle the respective channels and to arrive at conclusive evidence. On the other hand, with 2D spectroscopy as shown here, the different contributions are separated due to the second frequency axis (Figures 2 and 3), and thus one can directly read off the relevant photochemistry from the experimental 2D traces. Thus, the (qualitative) analysis is greatly simplified, even though three rather than two pulses have to be employed in the experiment. Hence, we believe that coherent 2D electronic spectroscopy holds great promise not only for analyzing photophysical processes such as energy transport but also for providing new insights into photochemical reactions with many (interconnected) pathways.

## AUTHOR INFORMATION

### Corresponding Author

*E-mail: brixner@phys-chemie.uni-wuerzburg.de.

## ACKNOWLEDGMENT

We are grateful to R. Schmidt and F. Würthner for fruitful discussions and the synthesis of 6,8-dinitro-BIPS. We thank the Deutsche Forschungsgemeinschaft (GRK 1221) for financial support.

## REFERENCES


(1) Feringa, B. L. *Molecular Switches*; Wiley-VCH: Berlin, 2001.
(2) Hobley, J.; Malatesta, V.; Millini, R.; Montanari, L.; Parker, W. O. N. *Phys. Chem. Chem. Phys.* **1999**, *1*, 3259–3267.
(3) Hobley, J.; Pfeifer-Fukumura, U.; Bletz, M.; Asahi, T.; Masuhara, H.; Fukumura, H. *J. Phys. Chem. A* **2002**, *106*, 2265–2270.
(4) Buback, J.; Kullmann, M.; Langhojer, F.; Nuernberger, P.; Schmidt, R.; Würthner, F.; Brixner, T. *J. Am. Chem. Soc.* **2010**, *132*, 16510–16519.
(5) Buback, J.; Nuernberger, P.; Kullmann, M.; Langhojer, F.; Schmidt, R.; Würthner, F.; Brixner, T. *J. Phys. Chem. A* **2011**, *115*, 3924–3935.
(6) Mukamel, S. *Principles of Nonlinear Optical Spectroscopy*; Oxford University Press, New York, 1999.
(7) Mukamel, S. *Annu. Rev. Phys. Chem.* **2000**, *51*, 691–729.
(8) Jonas, D. M. *Annu. Rev. Phys. Chem.* **2003**, *54*, 425–463.
(9) Cho, M. *Two-Dimensional Optical Spectroscopy*; CRC Press: Boca Raton, FL, 2009.
(10) Ogilvie, J. P.; Kubarych, K. J. *Adv. At. Mol. Opt. Phys.* **2009**, *57*, 249–321.
(11) Hamm, P.; Lim, M.; Hochstrasser, R. M. *J. Phys. Chem. B* **1998**, *102*, 6123–6138.
(12) Golonzka, O.; Khalil, M.; Demirdöven, N.; Tokmakoff, A. *Phys. Rev. Lett.* **2001**, *86*, 2154–2157.
(13) Hybl, J. D.; Albrecht, A. W.; Gallagher Faeder, S. M.; Jonas, D. M. *Chem. Phys. Lett.* **1998**, *297*, 307–313.
(14) Brixner, T.; Stiopkin, I. V.; Fleming, G. R. *Opt. Lett.* **2004**, *29*, 884–886.
(15) Cowan, M. L.; Ogilvie, J. P.; Miller, R. J. D. *Chem. Phys. Lett.* **2004**, *386*, 184–189.
(16) Selig, U.; Langhojer, F.; Dimler, F.; Löhrig, T.; Schwarz, C.; Gieseking, B.; Brixner, T. *Opt. Lett.* **2008**, *33*, 2851–2853.
(17) Tseng, C.; Matsika, S.; Weinacht, T. C. *Opt. Express* **2009**, *17*, 18788–18793.
(18) Selig, U.; Schleussner, C.; Foerster, M.; Langhojer, F.; Nuernberger, P.; Brixner, T. *Opt. Lett.* **2010**, *35*, 4178–4180.
(19) Bredenbeck, J.; Helbing, J.; Behrendt, R.; Renner, C.; Moroder, L.; Wachtveitl, J.; Hamm, P. *J. Phys. Chem. B* **2003**, *107*, 8654–8660.
(20) Hamm, P.; Helbing, J.; Bredenbeck, J. *Annu. Rev. Phys. Chem.* **2008**, *59*, 291–317.
(21) Chung, H. S.; Ganim, Z.; Jones, K. C.; Tokmakoff, A. *Proc. Natl. Acad. Sci. U.S.A.* **2007**, *104*, 14237–14242.
(22) Bredenbeck, J.; Helbing, J.; Kolano, C.; Hamm, P. *ChemPhysChem* **2007**, *8*, 1747–1756.
(23) Baiz, C. R.; Nee, M. J.; McCanne, R.; Kubarych, K. J. *Opt. Lett.* **2008**, *33*, 2533–2535.
(24) Zheng, J.; Kwak, K.; Asbury, J.; Chen, X.; Piletic, I. R.; Fayer, M. D. *Science* **2005**, *309*, 1338–1343.
(25) Kim, Y. S.; Hochstrasser, R. M. *Proc. Natl. Acad. Sci. U.S.A.* **2005**, *102*, 11185–11190.
(26) Woutersen, S.; Mu, Y.; Stock, G.; Hamm, P. *Chem. Phys.* **2001**, *266*, 137–147.
(27) Anna, J. M.; Ross, M. R.; Kubarych, K. J. *J. Phys. Chem. A* **2009**, *113*, 6544–6547.
(28) Olschewski, M.; Knop, S.; Seehusen, J.; Lindner, J.; Vöhringer, P. *J. Phys. Chem. A* **2011**, *115*, 1210–1221.
(29) Gallagher Faeder, S. M.; Jonas, D. M. *J. Phys. Chem. A* **1999**, *103*, 10489–10505.
(30) Grumstrup, E. M.; Shim, S.; Montgomery, M. A.; Damrauer, N. H.; Zanni, M. T. *Opt. Express* **2007**, *15*, 16681–16689.
(31) Shim, S.; Strasfeld, D. B.; Ling, Y. L.; Zanni, M. T. *Proc. Natl. Acad. Sci. U.S.A.* **2007**, *104*, 14197–14202.
(32) Myers, J. A.; Lewis, K. L.; Tekavec, P. F.; Ogilvie, J. P. *Opt. Express* **2008**, *16*, 17420–17428.
(33) Myers, J. A.; Lewis, K. L. M.; Fuller, F. D.; Tekavec, P. F.; Yocum, C. F.; Ogilvie, J. P. *J. Phys. Chem. Lett.* **2010**, *1*, 2774–2780.
(34) Tekavec, P. F.; Myers, J. A.; Lewis, K. L. M.; Ogilvie, J. P. *Opt. Lett.* **2009**, *34*, 1390–1392.
(35) Dürr, H.; Bouas-Laurent, H. *Photochromism: Molecules and Systems*; Elsevier: Amsterdam, 2003.
(36) Shim, S.; Zanni, M. T. *Phys. Chem. Chem. Phys.* **2009**, *11*, 748–761.
(37) Amat-Roldán, I.; Cormack, I.; Loza-Alvarez, P.; Gualda, E.; Artigas, D. *Opt. Express* **2004**, *12*, 1169–1178.
(38) Galler, A.; Feurer, T. *Appl. Phys. B: Laser Opt.* **2008**, *90*, 427–430.
(39) Ruhman, S.; Joly, A. G.; Nelson, K. A. *J. Chem. Phys.* **1987**, *86*, 6563–6565.
(40) Kovalenko, S. A.; Dobryakov, A. L.; Ruthmann, J.; Ernsting, N. P. *Phys. Rev. A* **1999**, *59*, 2369–2384.
(41) Megerle, U.; Pugliesi, I.; Schriever, C.; Sailer, C.; Riedle, E. *Appl. Phys. B: Laser Opt.* **2009**, *96*, 215–231.
(42) Tekavec, P. F.; Myers, J. A.; Lewis, K. L. M.; Fuller, F. D.; Ogilvie, J. P. *Opt. Express* **2010**, *18*, 11015–11024.
(43) Baraldi, I.; Momicchioli, F.; Ponterini, G.; Tatikolov, A. S.; Vanossi, D. *Phys. Chem. Chem. Phys.* **2003**, *5*, 979–987.
(44) Gómez, I.; Reguero, M.; Robb, M. A. *J. Phys. Chem. A* **2006**, *110*, 3986–3991.
(45) Wohl, C. J.; Kuciauskas, D. *J. Phys. Chem. B* **2005**, *109*, 22186–22191.